Hindawi
Advances in Materials Science and Engineering
Volume 2018, Article ID 6971981, 5 pages
https://doi.org/10.1155/2018/6971981

Research Article

Liquid Phase Separation Mechanism of Cu-40 wt.% Pb Hypermonotectic Alloys

Xiaosi Sun,[1] **Weixin Hao**,[1] **Teng Ma**,[1] **Junting Zhang**,[2] **and Guihong Geng**[3]

[1]*School of Materials Science and Engineering, Taiyuan University of Science and Technology, Taiyuan 030024, China*
[2]*School of Applied Science, Taiyuan University of Science and Technology, Taiyuan 030024, China*
[3]*School of Materials Science and Engineering, North Minzu University, Yinchuan 750000, China*

Correspondence should be addressed to Weixin Hao; wxhao@vip.sina.com and Guihong Geng; gengguihong@163.com

Received 25 January 2018; Revised 19 March 2018; Accepted 10 April 2018; Published 14 May 2018

Academic Editor: Guoqiang Xie

Solidification microstructures of Cu-40 wt.% Pb alloy were examined under different undercooling degrees. The liquid phase separation mechanism in the systems with stable miscibility gaps mainly involved Ostwald ripening, Brownian motion, Marangoni migration, and Stokes motion. Stokes had little influence on the liquid phase separation in the early phase and played a leading role in the later period. The liquid phase separation mechanism of Cu-40 wt.% Pb hypermonotectic alloy was illustrated in detail.

1. Introduction

Since Nakagawa [1] first detected the liquid phase separation in undercooled Cu-Fe and Cu-Co systems by magnetic methods in 1958, liquid immiscible alloys have been attracting wide attention from the researchers in materials science [2–4]. In the phase diagrams of these alloys (Cu-Pb monotectic alloy and Cu-Fe peritectic alloy), there is a stable or metastable liquid miscibility gap over a wide range of compositions. These immiscible alloys are easily transformed into seriously segregated microstructures under ordinary solidification conditions. Previous studies [5–7] revealed that two liquid phases with different compositions coexisted once the homogeneous alloy liquid was cooled into the miscibility gap. The globules of minority liquid phase were generated, and then they grew and migrated under a combined effect due to complex factors, including the Marangoni motion [8], Brownian motion [9], convective flow [10], gravity [11], wettability between the two liquid phases [12], and cooling rate [13]. Apparently, the seriously segregated microstructure of immiscible liquid alloys under normal ground conditions has greatly restricted their broad applications.

Monotectic alloy is a representative immiscible alloy. The study on its liquid phase separation mechanism might expand its application scope. If the second phase is homogeneously dispersed by an appropriate method, many potential special properties of the monotectic alloy [14] can be obtained for wide engineering applications. In previous studies on the liquid phase separation mechanism of monotectic alloys, L2 was generally treated as the primary phase in the initial stage of solidification, and the separation of liquid phase and the process of monotectic reaction were confused together. The study aims to explore the phase separation and formation of monotectic cells of monotectic alloy. Phase diagrams (Figure 1) of Cu-Pb monotectic alloys were obtained. In hypermonotectic alloys with the composition range of 37.4–86%, the liquid phase separation phenomenon occurred above the monotectic temperature. Therefore, in this study, the Cu-40 wt.% Pb hypermonotectic alloy was investigated, and its position in the phase diagram [15] was marked with the arrow (Figure 1).

2. Experiment

The specimens of Cu-Pb alloys with the desired compositions were prepared with high-purity Cu (99.99%) and Al (99.99%). In order to ensure that the cooling conditions of the specimen were the same, the weights of all the specimens were the same, 10 g. The experiment involved two steps. Firstly, the microstructure of Cu-40 wt.% Pb melt in the

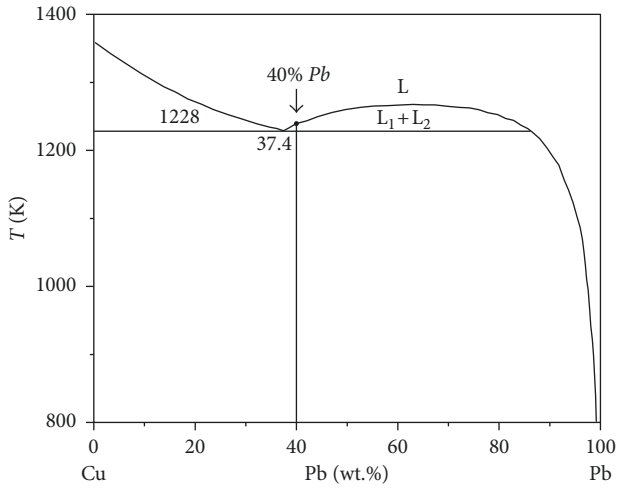

Figure 1: Phase diagrams of Cu-Pb monotectic alloys [15].

initial stage of liquid phase separation was observed. Secondly, the microstructures of Cu-40 wt.% Pb melt under different degrees of undercooling in the middle and late stages of liquid phase separation were observed.

2.1. Quenching on a Copper Chill Plate. First of all, the master alloy was melted by RF induction melting facility. Each specimen was placed in a quartz tube with a hole (diameter: 0.3 mm) in the center of its bottom, and its temperature was measured by an infrared thermometer. In this experiment, the infrared thermometer CIT-2MK2H produced by Beijing Sanbo Zhongzi Technology Co., Ltd., was used, and its response time was 1 ms. The pressure in the quartz tube was evacuated to 2×10^{-4} Pa and backfilled with 50% Ar + 50% He gas atmosphere to the pressure of about 100 kPa. When the melt temperature was lower than the liquid and higher than the monotectic reaction temperature, the power of the RF induction melting facility was cut off. Subsequently, the alloy melt was atomized into small droplets by jet stream through the nozzle. In the end, the solidified particles were quenched on a copper chill plate under the quartz tube.

2.2. Conventional Cooling. The thin scraps of saw metals were uniformly placed at the bottom of the crucible according to a predetermined distribution ratio, and then a certain amount of B_2O_3 glass was covered on the top surface. In order to avoid the further oxidation of the metal, after all the fine scraps were melted, the heat preservation was carried out for 3 to 5 min. When the degree of superheat of the melt was about 150 K, the specimen was cooled with the furnace and the cooling rate was 10 K·min^{-1}. After the solidification process was completed, the specimen was heated to the maximum degree of superheat. These procedures were repeated several times until the alloy achieved the desired undercooling. Then, the specimen was taken out.

The specimens were embedded into bakelite powder, abraded, polished, and corroded, and then the microstructure was analyzed by the 4xA HITACHI microscope and HITACHI S-3000N scanning electron microscope. The used etchant was 10% $FeCl_3$ + 10% HCl + 80% H_2O solution.

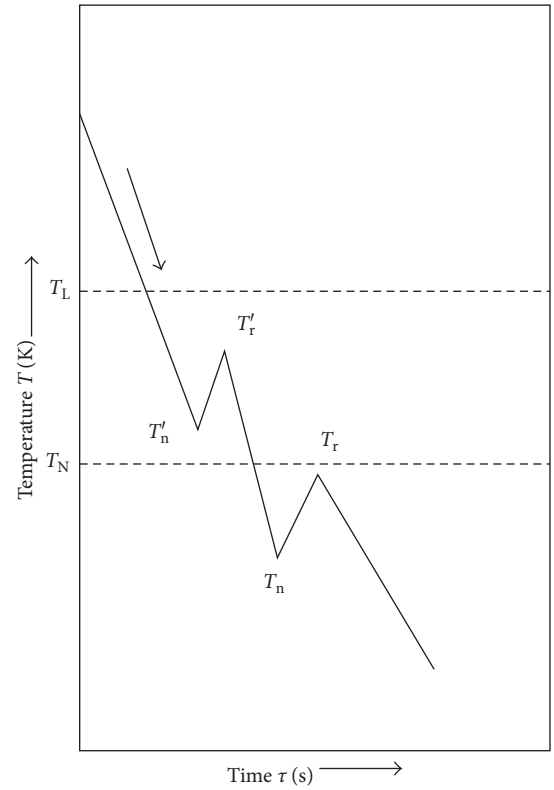

Figure 2: Cooling curves of the undercooled Cu-40 wt.% Pb alloy melt (T_L is liquidus and T_N is monotectic reaction temperature).

The microstructure, phase structure, phase transition process, and composition of the specimens were analyzed by the optical microscope, scanning electron microscope (SEM), and X-ray diffractometer (XRD), respectively. The phase structures of some specimens were analyzed on the Rigaka D/max-RB X-ray diffractometer produced by Japanese Science Company under the conditions of the scanning angle of 30°–85°, step size of 0.02°, and step time of 30 min.

3. Results and Discussion

3.1. Freezing Process. The cooling curve of hypermonotectic Cu-40 wt.% Pb alloy melt is shown in Figure 2. Recalescence occurred twice. Each recalescence corresponded to the formation of a new phase [16]. The first recalescence (T'_n-T'_r in Figure 2) indicated that the liquid phase separation occurred in the melt (L → L1 + L2). The result was confirmed by the microstructure of the quenched alloy melt (Figure 3). Spheres were observed (Figure 3), indicating that the liquid had entered the miscibility gap [6]. As shown in Figure 4, the sphere is the Cu-rich structure (L1), as indicated by the component analysis results. The structure may be interpreted as follows. The atomic volume of the solute Pb was larger than the atomic volume of the solvent Cu, thus distorting the crystal lattice of the solvent and increasing the potential energy. However, the system always proceeded spontaneously in the direction of decreasing the free energy because these larger atoms were always squeezed to the surface and enriched on the surface to form positive adsorption. The surface tension of the whole

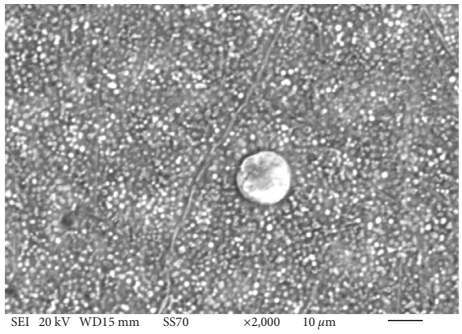

Figure 3: Microstructures of Cu-40 wt.% Pb hypermonotectic alloy under low undercooling.

system was reduced because of the large volume of these atoms and the low surface tension. Due to the efflux of solute Pb atoms, the internal solvent Cu atoms were rapidly enriched and nucleated, so the sphere structure of surface Pb-rich thin layer and internal rich Cu (L1) was formed (Figure 4). However, in view of the thermal behavior, since the nucleation of L1 and L2 proceeded in quick succession, the growth of one was prone to stimulate the growth of the other [7].

The second recalescence (T_n-T_r in Figure 2) indicated that the monotectic reaction occurred in the melt (L1 → α(Cu) + L2). The L1 phase was the product of the preferential nucleation in the monocrystalline reaction.

3.2. Formation Mechanism of Monotectic Cells. Figure 5 shows the solidification structure of undercooled Cu-40 wt.% Pb alloy at different degrees of undercooling. During the solidification process of low undercooling (40–75 K), the melt of the alloy underwent a liquid phase separation process. In the undercooled melt, the liquid phase of L2 (Pb) was distributed in the L1 (Cu) liquid phase. The monocrystalline reaction first occurred in the L1 sphere. The monotectic cell grew along the direction of the heat release, so the formed α(Cu) grew in the form of fibrous and formed the radial pattern in the rapid solidification stage. The enriched L2 phase was distributed between α(Cu) and formed a metamorphic chrysanthemum-like structure.

At the same time, the residual L1 after recalescence generated L2 phase between fibrous α(Cu) in the monotectic reaction. When the temperature decreased to 599 K, the eutectic reaction occurred in L2. The formed metamorphic cells were distributed uniformly in the solidified structure and the granular and fibrous Pb diffused on the S (Cu)-based substrates (Figure 5(a)). With the increase in the undercooling degree, the number of formed metamorphic cells increased continuously and the growth of the metamorphic cell was accelerated. As a result, adjacent metamorphic cells were bound to each other and irregular metamorphic cells were formed in the solidified structure (Figure 5(b)). When the undercooling reached 80 K, the macrosegregation of Pb appeared obviously in the solidification microstructure (Figure 5(c)). With the increase in the undercooling degree, the stratification phenomenon finally appeared in the solidified microstructure (Figure 5(d)).

3.3. Organization Evolution. Within the small undercooling range, the large solubility was promoted by small droplet radius [17], and the low viscosity and large diffusion coefficient were caused by low undercooling, thus allowing Ostwald ripening [4]. Moreover, migration or coagulation did not occur within short time interval Δt due to the low undercooling. Therefore, the coarsening of L1 droplets within the undercooling range should be ascribed to Ostwald ripening.

With the decrease in temperature and the increase in droplet radius, the solid-liquid interfacial tension increased gradually and the solubility decreased, thus weakening Oswald ripening. At this time, the increased time interval Δt was enough to support the condensation and collision of droplets, in which the main mechanisms included Brownian motion, Marangoni migration, and Stokes motion. The SEM images illustrate a characteristic microstructure of Cu-40 wt.% Pb hypermonotectic alloys under different undercooling degrees in Figure 5. For the undercooling degree of 42 K, as shown in Figure 5(a), some chrysanthemum-like structures consisting of two liquids occur in the matrix. One is the white Cu-rich (L1) phase, and the other is the black Pb-rich (L2) phase. As shown in Figure 5(a), the outermost layer of chrysanthemum-like structure is L2 because the surface energy of L2 is lower than that of L1. There is still partial L2 diffused in the center of the chrysanthemum-like structure due to the solute retention caused by rapid solidification of α(Cu) to L2. With the increase in undercooling, the cooling rate is accelerated. Therefore, the solidification rate of α(Cu) is accelerated and the solute retention of L2 is more obvious, as shown in Figure 5(b).

In the early stage of liquid phase separation, due to the small size of chrysanthemum-shaped droplets, Stokes motion was not obvious, as confirmed by (1) and (2) [18]. As shown in Figure 5(b), some L2 Pb-rich phases form larger particles through collision and coagulation, and the separation process is more complete than that shown in Figure 5(a). With the increase in undercooling and the increase in the volume of the minority phase of L2 particles, the influence of Stokes motion was gradually enhanced until v_s was much larger than v_m. At this point, the Stokes motion had a dominant effect on the particles [19]. The results showed that the Pb-rich phase of L2 with the high density grew rapidly and sank and the matrix L1 Cu-rich phase migrated to the upper specimen due to the action of buoyancy (Figure 5(c)). In the later stage of liquid phase separation, with the obvious growth of the radius of the spherule, the Stokes motion was more obvious. At the same time, the undercooling degree was increased, and the Stokes motion rate was increased obviously [20], thus accelerating the increase in the sphere radius. As a result, the liquid phase separation tended to be seriously segregated, indicating the phenomenon of delamination (Figure 5(d)).

$$v_m \approx \frac{-2r}{3(3\mu_d + 2\mu_m)} \cdot \frac{\partial \sigma}{\partial T} \cdot \frac{\partial T}{\partial x}, \quad (1)$$

$$v_s \approx \frac{2g\Delta\rho r^2}{3\mu_m} \cdot \frac{\mu_d + \mu_m}{3\mu_d + 2\mu_m}, \quad (2)$$

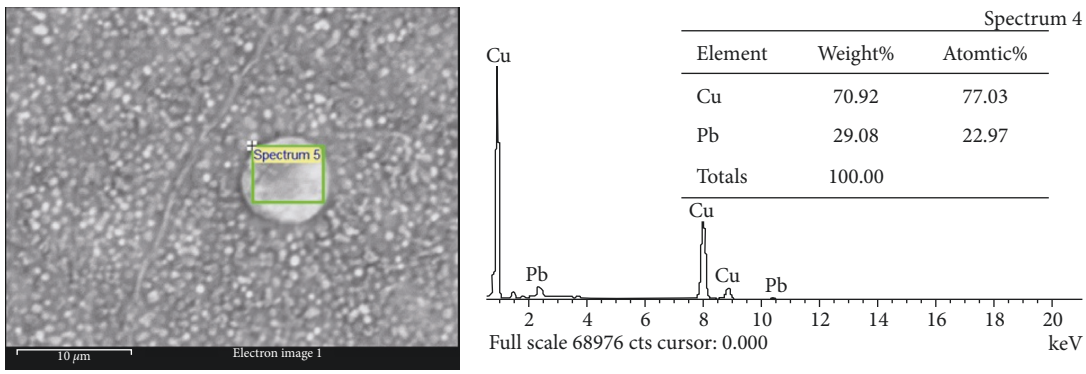

(a) (b)

Figure 4: Energy spectrum of Cu-40 wt.% Pb hypermonotectic alloy under low undercooling.

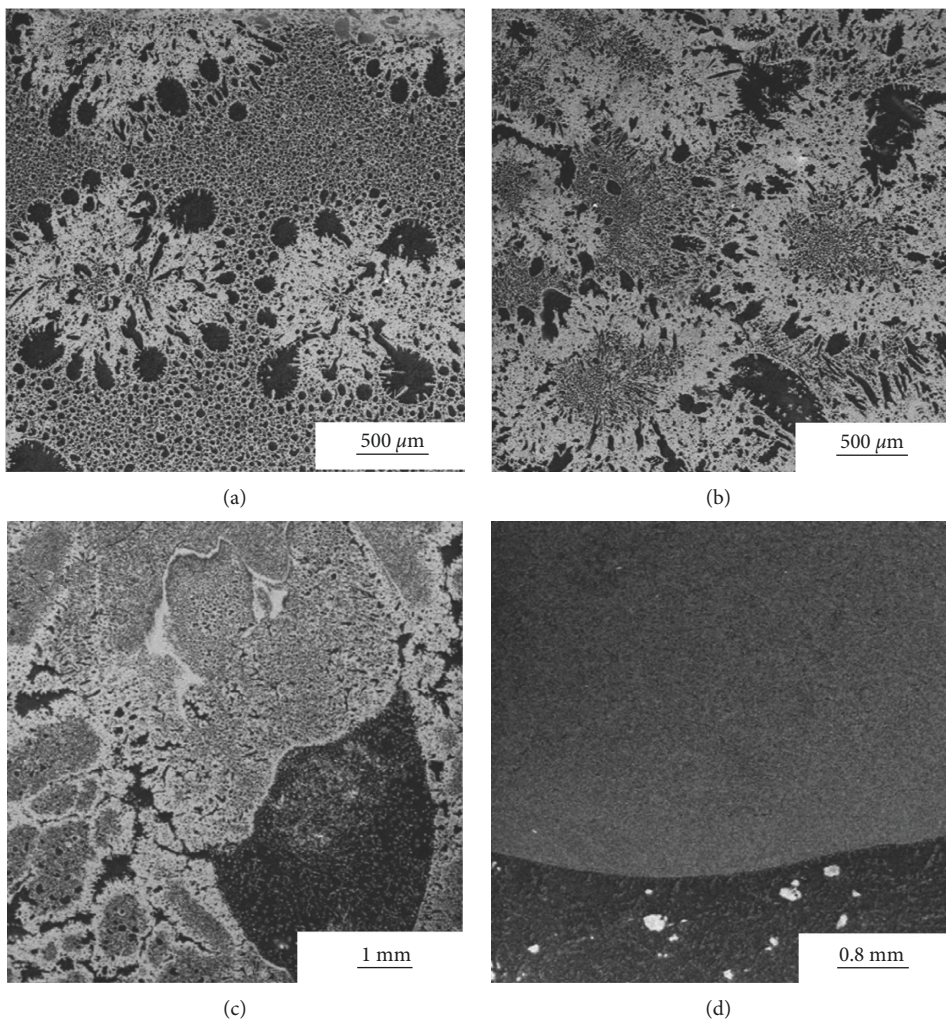

(a) (b)

(c) (d)

Figure 5: Microstructures of Cu-40 wt.% Pb hypermonotectic alloy under different degrees of undercooling: (a) $\Delta T = 42$ K; (b) $\Delta T = 65$ K; (c) $\Delta T = 80$ K; (d) $\Delta T = 142$ K.

where r is the diameter of the globule, μ_d and μ_m are respectively the viscosities of the globule and matrix, σ is the interfacial energy, x is the distance, g is the gravity coefficient, and $\Delta\rho$ is the density difference between the globule and matrix.

4. Conclusions

The microstructures of Cu-40 wt.% Pb alloy during liquid phase separation under different undercooling degrees were obtained by experiments. The liquid phase

separation mechanisms were described in detail. The results were summarized below:

(a) The nucleation process of L1 and L2 in the initial stage of liquid phase separation before the monotectic reaction of hypermonotectic alloy was first expounded in detail. The result was completely different from the previous study in which the liquid phase separation was confused with the monotectic reaction and the default L2 was the preferential nucleation phase. L1 phase nucleation was prior to L2 phase nucleation, and the nucleation of L1 and L2 proceeded in quick succession.

(b) The formation mechanism of monotectic cells was described in detail. That is, α(Cu) which is generated in the metamorphic reaction grew in the form of fibrous and formed the radial pattern in the rapid solidification stage. The enriched L2 phase was distributed between α(Cu) and formed a metamorphic chrysanthemum-like structure.

(c) In the early stage of liquid phase separation, Brownian motion and Martini migration played the dominant role, whereas Stokes motion was the main controlling factor in the later stage.

Data Availability

The data used to support the findings of this study are available from the corresponding author upon request.

Conflicts of Interest

The authors declare that they have no conflicts of interest.

Acknowledgments

This work was cofinanced by the National Natural Science Foundation of China (Grant nos. 51561001 and 51641406).

References

[1] Y. Nakagawa, "Liquid immiscibility in copper-iron and copper-cobalt systems in the supercooled state," *Acta Metallurgica*, vol. 6, no. 11, pp. 704–711, 1958.

[2] G. K. Shrestha, B. K. Singh, I. S. Jha, and I. Koirala, "Theoretical study of thermodynamic properties of Cu-Pb liquid alloys at different temperature by optimization method," *Journal of Institute of Science and Technology*, vol. 22, no. 1, pp. 25–33, 2017.

[3] D. Mirkovic, J. Grobner, and R. Schmid-Fetzer, "Solidification paths of multicomponent monotectic aluminum alloys," *Acta Materialia*, vol. 56, no. 18, pp. 5214–5222, 2008.

[4] Y. Z. Chen, F. Liu, G. C. Yang, X. Q. Xu, and Y. H. Zhou, "Rapid solidification of bulk undercooled hypoperitectic Fe–Cu alloy," *Journal of Alloys and Compounds*, vol. 427, no. 1-2, pp. L1–L5, 2007.

[5] Z. Q. Kang, Y. B. Zhang, X. Yang, G. H. Feng, and L. Zhang, "Numerical study on the impact of second phase content on the solidification of Al-Pb hypermonotectic alloys," *Materials Science Forum*, vol. 896, pp. 209–215, 2017.

[6] A. Munitz, A. Venkert, P. Landau, M. J. Kaufman, and R. Abbaschian, "Microstructure and phase selection in supercooled copper alloys exhibiting metastable liquid miscibility gaps," *Journal of Materials Science*, vol. 47, no. 23, pp. 7955–7970, 2012.

[7] N. Liu, G. C. Yang, W. Yang, F. Liu, C. L. Yang, and Y. H. Zhou, "Microstructure evolution of undercooled Fe–Co–Cu alloys," *Physica B Physics of Condensed Matter*, vol. 406, no. 4, pp. 957–962, 2011.

[8] W. Q. Lu, S. G. Zhang, W. Zhang et al., "A full view of the segregation evolution in Al–Bi immiscible alloy," *Metallurgical and Materials Transactions A*, vol. 48, no. 6, pp. 2701–2705, 2017.

[9] J. Z. Zhao, "The kinetics of the liquid–liquid decomposition under the rapid solidification conditions of gas atomization," *Materials Science and Engineering: A*, vol. 454-455, pp. 637–640, 2007.

[10] H. L. Li, J. Z. Zhao, Q. X. Zhang, and J. He, "Microstructure formation in a directionally solidified immiscible alloy," *Metallurgical and Materials Transactions A*, vol. 39, pp. 3308–3316, 2008.

[11] A. P. Silva, J. E. Spinelli, and A. Garcia, "Microstructural evolution during upward and downward transient directional solidification of hypomonotectic and monotectic Al–Bi alloys," *Journal of Alloys and Compounds*, vol. 480, no. 2, pp. 485–493, 2009.

[12] J. Z. Zhao, T. Ahmed, H. X. Jiang, J. He, and Q. Sun, "Solidification of immiscible alloys: a review," *Acta Metallurgica Sinica*, vol. 30, no. 1, pp. 1–28, 2017.

[13] C. P. Wang, X. J. Liu, Y. Takaku, I. Ohnuma, R. Kainuma, and K. Ishida, "Formation of core-type macroscopic morphologies in Cu-Fe base alloys with liquid miscibility gap," *Metallurgical and Materials Transactions A*, vol. 35, no. 4, pp. 1243–1253, 2004.

[14] L. Wang, S. S. Li, L. Bo, D. Wu, and D. G. Zhao, "Liquid-liquid phase separation and solidification behavior of Al-Bi-Sn monotectic alloy," *Journal of Molecular Liquids*, vol. 254, pp. 333–339, 2018.

[15] N. Wang, L. Zhang, and Y. P. Zheng, "Shell phase selection and layer numbers of core–shell structure in monotectic alloys with stable miscibility gap," *Journal of Alloys and Compounds*, vol. 538, no. 538, pp. 224–229, 2012.

[16] D. L. Li, G. C. Yang, and Y. H. Zhou, "A new approach to preparing three-dimensional amorphous alloys," *Journal of Materials Science Letters*, vol. 11, no. 15, pp. 1033–1035, 1992.

[17] J. R. Rogers and R. H. Davis, "Modeling of collision and coalescence of droplets during microgravity processing of Zn-Bi immiscible alloys," *Metallurgical Transactions A*, vol. 21, no. 1, pp. 59–68, 1990.

[18] L. Ratke and P. W. Voorhees, *Growth and Coarsening: Ostwald Ripening in Material Processing*, Springer-Verlag, New York, NY, USA, 2002.

[19] R. Dai, S. G. Zhang, Y. B. Li, X. Guo, and J. G. Li, "Phase separation and formation of core-type microstructure of Al–65.5 mass% Bi immiscible alloys," *Journal of Alloys and Compounds*, vol. 509, no. 5, pp. 2289–2293, 2011.

[20] N. Liu, "Investigation on the phase separation in undercooled Cu–Fe melts," *Journal of Non-Crystalline Solids*, vol. 358, no. 2, pp. 196–199, 2012.